Journal of Inorganic Biochemistry 202 (2020) 110870

Contents lists available at ScienceDirect

Journal of Inorganic Biochemistry

journal homepage: www.elsevier.com/locate/jinorgbio

Pt(II) and Pd(II) complexes with a thiazoline derivative ligand: Synthesis, structural characterization, antiproliferative activity and evaluation of pro-apoptotic ability in tumor cell lines HT-29 and U-937☆

Elena Fernández-Delgado[a], Felipe de la Cruz-Martínez[b], Carmen Galán[a], Lourdes Franco[a], Javier Espino[a], Emilio Viñuelas-Zahínos[b], Francisco Luna-Giles[b,*], Ignacio Bejarano[c,*]

[a] Department of Physiology (Neuroimmunophysiology and Chrononutrition Research Group), University of Extremadura, 06006 Badajoz, Spain
[b] Department of Organic and Inorganic Chemistry (Coordination Chemistry Group), University of Extremadura, 06006 Badajoz, Spain
[c] Department of Physiology and Pharmacology, University of Cantabria, 39011 Santander, Spain

ARTICLE INFO

Keywords:
Apoptosis
Thiazoline
Pd(II) and Pt(II) complexes
Tumor cells
U-937
HT-29

ABSTRACT

Eluding apoptosis represents the hallmark of tumoral cell behavior. Cisplatin (CisPt) is a very common chemotherapeutic agent to treat cancer by reestablishing apoptotic mechanisms of cell death. However, certain patients acquire resistance to CisPt as well as suffer nephrotoxicity, neurotoxicity, nausea and vomiting. The synthesis of new Pt(II) compounds represents an alternative to CisPt to avoid resistance and undesirable side effects. Pd(II) could be a Pt(II) surrogate given the similarity of coordination chemistry between them, thus widening the spectra of available anticancer drugs. Herein, we have synthesized and characterized two Pt(II) or Pd(II) complexes with TdTn (2-(3,4-dichlorophenyl)imino-N-(2-thiazolin-2-yl)thiazolidine), a thiazoline derivative ligand, with formula [$PtCl_2$(TdTn)] and [$PdCl_2$(TdTn)]. The potential anticancer ability was evaluated in human colon adenocarcinoma HT-29 and human histiocytic lymphoma U-937 cell lines. To that aim, U-937 and HT-29 cells were treated with TdTn, [$PtCl_2$(TdTn)] and [$PdCl_2$(TdTn)] for 24 h. The microscopy monitoring indicated that TdTn, [$PtCl_2$(TdTn)] and [$PdCl_2$(TdTn)] arrested the cell proliferation of U-937 and HT-29 cells with respect to control, in agreement with MTT (3-[4,5-dimethylthiazole-2-yl]-2,5-diphenyltetrazolium bromide) analysis. Moreover, it is noteworthy that the ligand by its own showed antiproliferative effects in both cell lines. [$PtCl_2$(TdTn)] and [$PdCl_2$(TdTn)] caused caspase-3 activation in U-937 cells, simultaneously with caspase-9 activation due to complexes; however, in HT-29 caspase-3 activation occurred simultaneously with caspase-8 activation induced by the ligand TdTn. Only metal complexes were able to induce ROS (Reactive Oxygen Species) generation in U-937 cells, but not TdTn. In HT-29 cells neither the metal complexes, nor the ligand induced ROS generation.

1. Introduction

Evasion of apoptosis is considered one of the main hallmarks of cancer [1] and may favor tumor progression and contributes to treatment resistance [2]. It is known that by 2015, 8.8 million people died from cancer and the number of new cases is expected to rise by about 70% in the next 20 years. Nowadays pulmonary, hepatic, colorectal, gastric and breast cancers are considered the deadliest cancers [3]. Colorectal cancer occurs in the colon or rectum and most of this type of cancer are adenocarcinomas. According to the International Agency for Research of Cancer (IARC), the mortality in 2012 of colorectal cancer reached 693,933 people [4].

Among acute leukemias, acute myeloid leukemia (AML) is the most common type and it causes a high mortality [5]. The estimated number of deaths worldwide, due to leukemia is 265,471 people in 2012 [4]. In the case of AML, although in most patients a complete remission of the disease is achieved, it should be noted that many of them suffer a relapse due to resistance to chemotherapy. Because of this, avoiding chemoresistance in leukemia has become one of the main goals nowadays for researches in this field [6].

Cisplatin (CisPt) is one of the most common chemotherapeutic agents to treat tumor cells, including AML and colorectal cancer. Unfortunately, in some cases the use of CisPt is limited because of the intrinsic or acquired resistance of different types of cancer. At the same

☆ This manuscript is in Memoriam Prof. Juan Manuel Salas Peregrín.

* Corresponding authors.
E-mail addresses: pacoluna@unex.es (F. Luna-Giles), bejaranoi@unican.es (I. Bejarano).

https://doi.org/10.1016/j.jinorgbio.2019.110870
Received 15 May 2019; Received in revised form 24 September 2019; Accepted 27 September 2019
Available online 22 October 2019
0162-0134/

time, the side effects that CisPt causes in patients such as nephrotoxicity, neurotoxicity, nausea and vomiting should be reduced ideally [7]. Therefore, these are the main reasons why there is still an intense research focussed on new compounds to be used in lower therapeutic doses with milder side effects. In the last 30 years, 23 platinum drugs have been tested in clinical trials, but only two of them have been authorized for clinical use worldwide: diamine (1,1-cyclobutadicarboxylato)platinum(II) (carboplatinum) and (1R,2R)-diaminocyclohexanooxalatoplatinum(II) (oxaliplatinum) [8].

Once CisPt is inside the cell, it is hydrolyzed giving rise to a highly reactive compound, $[PtCl(H_2O)(NH_3)_2]^+$, which rapidly induces intra- or inter-chain cross-links in the DNA, forming the so-called CisPt-DNA adducts [9]. These processes cause the inhibition of DNA replication, which confers its cytostatic power, especially in cancer cells, avoiding the constant synthesis of DNA needed by tumor cells to grow and end up causing apoptosis [10].

Among the many processes believed to be involved in resistance to CisPt, some of the most important ones involve reduced absorption of CisPt. The human copper transporter 1 (CTR1) has been found to be the main entry for CisPt, through a mechanism that mimics copper entry [11]. In this regard, expression of CTR1 (responsible for regulating intracellular copper homeostasis) has been shown to be reduced in a CisPt-resistant lung cancer line [12]. By contrast, in oral squamous cell carcinoma cells, no differences were found between the resistant line and the sensitive line, so that CTR1 may participate in the resistance of only certain types of tumors [13].

Other types of resistance mechanisms have been described to be involved in platinum drugs resistance, as an increased activity of nucleotide excision repair (NER) system [14]. NER repairs DNA by removing DNA adducts [15] such as Pt-DNA. There is a great deal of evidence that, among all the proteins involved in this repair system, overexpression of DNA excision repair protein ERCC1 (Excision repair complementing defective in Chinese hamster 1) is critical in CisPt resistance [16]. In patients with gastric tumors, a higher level of ERCC1 expression has been found in those with resistance to treatment [17]. In other types of tumors, such as ovarian cancer [18], non-small cell lung cancer [19] and testicular germ cell cancer, similar results have been obtained [20].

Besides, the inactivation of CisPt is considered another remarkable contribution to the CisPt resistance. Once the CisPt is hydrolyzed in the cytosol interacts with nucleophilic centers of endogenous molecules such as glutathione (GSH), methionine and some proteins. Thus, once CisPt enters the cell it can be inactivated by these interactions [21]. Some tumor cell lines resistant to CisPt, such as the A549/CDDP lung carcinoma line, have been found to possess higher levels of GSH and, therefore, accumulate less drug than sensitive lines, such as A549 cell line [22].

Thus, the synthesis of new Pt(II) compounds similar to CisPt might eliminate the problems derived from CisPt resistance. These compounds can be obtained introducing bioactive ligands in its structure as those that contain heterocycles with donor atoms. Among these heterocycles, thiazolines are five-membered heterocycles derived from thiazole containing an N atom and an S atom, in addition to a double bond. Depending on the relative position of the double bound, thiazolines are classified as 2-thiazolines, 3-thiazolines, 4-thiazolines and tetrahydrothiazoles or thiazolidines. It should be noted that thiazoles and thiazolines have been found in the structure of natural products of marine origin with anticancer activity such as tantazoles [23]. Also, synthetic oligomers derived from 2-thiazoline have been synthesized and inhibit cell growth in pancreatic, prostate and colonic cancer [24]. Furthermore, it is known that some synthetic derivatives containing the 2-thiazoline ring exhibit antitumor activity [25,26]. Additionally, Onen-Bayram et al. [27] found a new compound designed based on a thiazolidine ring that trigger caspase-9 dependent apoptosis in liver cancer cells and Romagnoli et al. [28] have observed that novel hybrid molecules containing 5-benzylidene thiazolidine-2,4-dione induce apoptosis in U-937 cells.

On the other hand, several metal complexes with antitumoral properties containing 2-thiazoline derivative ligands in their structures coordinated to metal atoms through the thiazoline nitrogen atoms have been described. Thus, Bolos et al. [29] and Chaviara et al. [30] have reported mixed ligand copper(II) complexes that present a 2-amino-2-thiazoline ligand inside the coordination sphere which shows antitumoral activity. Likewise, Dehand et al. [31] have studied Pt(II) and Pd(II) complexes with 2-mercaptothiazoline as ligand in acidic medium which appear to have a significant cytotoxic effect against hepatoma cells.

The development of metal coordination compounds with Pt(II) being the central metal ion has promoted the synthesis of new metallodrugs with antitumoral activity. However, in recent years several Pd(II) complexes showing important cytotoxic properties have been synthesized due to the similarity of coordination chemistry between Pt(II) and Pd(II) metal ions [32,33].

Therefore, in this work, it has been carried out the synthesis, structural characterization and evaluation of pro-apoptotic ability in tumor cells of Pt(II) and Pd(II) coordinated with TdTn (2-(3,4-dichlorophenyl)imino-N-(2-thiazolin-2-yl)thiazolidine), a polydentate thiazoline derivative ligand with contrasting coordinating ability [34–36]. Herein, we aim to study the potential anticancer ability in HT-29 and U-937 cell lines of TdTn compounds, which incorporate a metal center of Pt(II) or Pd(II) into their bioactive heterocycles.

2. Material and methods

2.1. General procedures

All reagents were commercial grade material and were used without further purification. Ligand 2-(3,4-dichlorophenyl)imino-*N*-(2-thiazolin-2-yl)thiazolidine (TdTn) [37] and precursor $[PtCl_2(DMSO)_2]$ [38] were prepared as described in the literature.

Chemical analysis of carbon, hydrogen, nitrogen and sulphur were performed by microanalytical methods using a Leco CHNS-932 or a Thermo Finnigan Flash 1112 microanalyzers. IR spectra were recorded on a Perkin-Elmer FT-IR 1720 spectrophotometer, from KBr pellets in the 4000–370 cm^{-1} range and on a Perkin-Elmer FT-IR 1700× spectrophotometer, from Nujol mulls in the 500–150 cm^{-1} range. ^1H NMR spectra were obtained with a Bruker Avance 500 instrument at 500 MHz at high temperature (330 K) in DMF-d_7, due to low solubility of complexes. ^1H NMR signals were referenced to residual proton resonances in deuterated solvents. ^{13}C NMR spectra have not been carried out due to the low solubility of complexes in DMF-d_7. ESI-MS were carried out with an Agilent Q-TOF instrument in methanol: DMSO (10:1) with addition of formic acid.

2.2. Preparation of $[PtCl_2(TdTn)]$ (PtTdTn)

A solution of TdTn (166 mg, 0.5 mmol) in ethanol (30 mL) was added drop by drop to a solution of $[PtCl_2(DMSO)_2]$ (211 mg, 0.5 mmol) in hot ethanol (40 mL) and the mixture was refluxed overnight. Then, the resulting yellow solid was filtered off and washed with water and cold ether. Yellow solid was recrystallized in dimethylformamide at 70 °C. After 24 h, yellow crystals were isolated from the solution. The crystals were separated by filtration, washed with cold ether and air-dried (237 mg, 79%). Anal. Calc. (%) for $C_{12}H_{11}Cl_4N_3PtS_2$: C, 24.09; H, 1.85; N, 7.02; S, 10.72%. Found: C, 24.26; H, 1.79; N, 7.02; S, 10.73%. IR (KBr): ν(C=N) 1607, (thiazoline ring vibrations) 1552, 965, 922, 778, 743, 629, 594, (thiazolidine ring vibrations) 1033, 922, 834, 700, 673, 486, 416, (metal-ligand vibrations) 441, 320, 258, 215 cm^{-1}. ^1H NMR (500 MHz, DMF-d_7, 330 K) δ 7.57 (d, J = 8.5 Hz, 1H, C(11)H), 7.28 (d, J = 2.5 Hz, 1H, C(12)H), 7.05 (dd, J = 8.5 Hz, J = 2.5 Hz, 1H, C(8)H), 4.68 (t, J = 7.2 Hz, 2H, C(5)H_2), 4.67 (t, J = 8.2 Hz, 2H, C(2)H_2), 3.58 (t, J = 8.2 Hz, 2H, C(3)

H_2), 3.52 (t, J = 7.2 Hz, 2H, C(6)H_2) ppm. ESI-MS 620.862 $[M + Na]^+$.

2.3. Preparation of [$PdCl_2$(TdTn)] (PdTdTn)

To a solution of $Na_2[PdCl_4]\cdot H_2O$ (157 mg, 0.5 mmol) in ethanol (5 mL) was added an ethanol solution (30 mL) of TdTn (166 mg, 0.5 mmol) and the mixture was refluxed overnight. Then, the resulting orange solid was filtered off and washed with water and cold ether. Orange solid was redissolved in dimethylformamide at 70 °C and allowed to evaporate slowly. After 24 h, orange crystals were isolated from the solution. The crystals were separated by filtration, washed with cold ether and air-dried (271 mg, 90%). Anal. Calc. (%) for $C_{12}H_{11}Cl_4N_3PdS_2\cdot 0.5H_2O$: C, 27.79; H, 2.33; N, 8.10; S, 12.36%. Found: C, 27.56; H, 2.59; N, 8.08; S, 11.99%. IR (KBr): ν(C═N) 1612, (thiazoline ring vibrations) 1547, 959, 919, 771, 729, 630, 591, (thiazolidine ring vibrations) 1030, 919, 833, 698, 671, 483, 414, (metal-ligand vibrations) 439, 322, 256, 217 cm^{-1}. ^{1}H NMR (500 MHz, DMF-d_7, 330 K) δ 7.54 (d, J = 8.5 Hz, 1H, C(11)H), 7.29 (d, J = 2.5 Hz, 1H, C(12)H), 7.06 (dd, J = 8.5 Hz, J = 2.5 Hz, 1H, C(8)H), 4.63 (t, J = 7.0 Hz, 2H, C(5)H_2), 4.53 (t, J = 8.0 Hz, 2H, C(2)H_2), 3.59 (t, J = 8.0 Hz, 2H, C(3)H_2), 3.54 (t, J = 7.0 Hz, 2H, C(6)H_2) ppm. ESI-MS 532.035 $[M + Na]^+$.

2.4. X-ray diffraction

The experimental details of the crystal structure determination, including crystal data, data collection, structure determination and refinement are listed in Table 1 for the complexes PtTdTn and PdTdTn. X-ray single-crystal diffraction measurements were performed using a Bruker Kappa APEXII CCD diffractometer with Mo-Kα radiation (λ = 0.71073 Å, graphite monochromator). All data were corrected for Lorentz and polarization effects, while absorption corrections were performed by means of SADABS [39] program. The structures were solved by direct methods and subsequent Fourier differences using the SHELXS-14 [40] program and refined by full-matrix least-squares on F^2 with SHELXL-18 [41], included in WINGX [42] package assuming anisotropic displacement parameters for non-hydrogen atoms. All hydrogen atoms attached to carbon atoms were positioned geometrically, with U_{iso} values derived from U_{eq} values of the corresponding carbon and nitrogen atoms. Crystallographic data for complexes PtTdTn and PdTdTn have been deposited at the CCDC (Cambridge Crystallographic Data Center; copies of the data can be obtained, e-mail: deposit@ccdc.cam.ac.uk or www: http://www.ccdc.cam.ac.uk) with CCDC numbers 1897293 and 1897294.

Table 1
Crystal data, data collection and refinement details for PtTdTn and PdTdTn.

	PtTdTn	PdTdTn
Crystal shape	Prism	Prism
Color	Yellow	Orange
Size (mm)	0.44 × 0.24 × 0.12	0.35 × 0.18 × 0.10
Chemical formula	$C_{12}H_{11}Cl_4N_3PtS_2$	$C_{12}H_{11}Cl_4N_3PdS_2$
Formula weight	598.25	509.56
Crystal system	Triclinic	Triclinic
Space group	P-1	P-1
Unit cell dimensions		
a (Å)	8.9894(3)	8.971(5)
b (Å)	9.0013(3)	9.039(5)
c (Å)	11.4059(4)	11.497(5)
α (°)	101.627(2)	76.613(5)
β (°)	90.517(2)	89.317(5)
γ (°)	110.844(2)	69.446(5)
Cell volume (Å^3)	841.53(5)	846.7(8)
Z	2	2
D_{calc} (g cm^{-3})	2.361	1.999
μ (mm^{-1})	9.216	1.970
F(000)	564	500
θ range	1.83–28.38	1.83–28.32
Index ranges	−10 ≤ h ≤ 12, −11 ≤ k ≤ 12 -15 ≤ l ≤ 15	−11 ≤ h ≤ 11, −11 ≤ k ≤ 12 −14 ≤ l ≤ 15
Temperature	170	298
Independent reflections	4166	3884
Observed reflections	4079[F > 4.0 σ(F)]	3662[F > 4.0 σ(F)]
Max/min transmission	0.7457/0.3549	0.7457/0.6067
No. of refined parameters	199	199
R [F > 4.0 σ(F)][a]	0.0248	0.0256
wR [F > 4.0 σ(F)][b]	0.0631	0.0639
GOF[c]	1.257	1.039
ρ_{max}, ρ_{min} (e Å^{-3})	1.960, −2.725	0.875, −1.340

[a] $R = \Sigma\,||F_o| - |F_c||/\Sigma\,|F_o|$.
[b] $R = \{\Sigma[w(F_o^2 - F_c^2)^2]/\Sigma\,[w(F_o^2)^2]\}^{1/2}$
[c] The goodness-of-fit(GOF) equals $\{\Sigma[w(F_o^2 - F_c^2)^2]/(N_{rflns} - N_{params})\}^{1/2}$.

For Powder X-ray diffraction, the powders of samples were gently ground in an agate mortar and then deposited with care in the hollow of an aluminum holder equipped with a zero-background plate. Diffraction data (Cu Kα, λ = 1.5418 Å) were collected on a θ:θ Bruker AXS D8 vertical scan diffractometer equipped with primary and secondary Soller slits, a secondary beam curved graphite monochromator, a Na(Tl)I scintillation detector, and pulse height amplifier discrimination. The generator was operated at 40 kV and 40 mA. Optics used are the following: divergence 0.5°, antiscatter 0.5°, receiving 0.2 mm. A long scan was performed with 5 < 2θ < 25° with t = 5 s and Δ2θ = 0.02°.

2.5. Reagents for biological studies

HT-29 cell line (ECACC No. 91072201) derived from human colon adenocarcinoma and U-937 cell line (ECACC No. 85011440) derived from human Caucasian histiocytic lymphoma were purchased from The European Collection of Cell Cultures (ECACC) (Dorset, UK). Fetal bovine serum (FBS) and penicillin/streptomycin were acquired from HyClone (Aalst, Belgium). L-Glutamine, RPMI (Roswell Park Memorial Institute) 1640 and Dulbecco's Modified Eagle medium (DMEM) were obtained from Lonza (Basel, Switzerland). Cisdiammineplatinum (II) dichloride (cisplatin), 4-(2-hydroxyethyl)-1-piperazineethanesulfonic acid (HEPES), 3-[(3-Cholamidopropyl)dimethylammonio]-1-propanesulfonate (CHAPS) hydrate, 4-Morpholineethanesulfonic acid (MES) hydrate, dithiothreitol (DTT), Poly(ethylene glycol) (PEG), Nonidet P 40 Substitute (NP40) *N*-acetyl-Asp-Glu-Val-Asp-7-amino-4-methylcoumarin (AC-DEVD-AMC), 3-(4,5-dimethylthiazol-2-yl)-2,5-diphenyltetrazolium bromide (MTT) were bought from Sigma Aldrich (Madrid, Spain). 2′,7′-Dichlorofluorescin diacetate (H2DCFDA) was acquired from Invitrogen (Barcelona, Spain). *N*-acetyl-Ile-Glu-Pro-Asp-7-amino-4-methylcoumarin (Ac-IEPD-AMC) and *N*-acetyl-Leu-Glu-His-Asp-7-amino-4-methylcoumarin (Ac-LETD-AMC) were purchased from Bachem (Bubendorf, Switzerland). All other reagents were of analytical grade.

2.6. Cell culture

HT-29 and U-937 cells were grown in DMEM and RPMI1640, respectively supplemented with 2 mM L-glutamine, 10% heat-inactivated FBS, 100 U/mL penicillin, and 10 μg/mL streptomycin. Cells were cultured under a humidified atmosphere containing 95% air and 5% CO_2 at 37 °C. U-937 cells were routinely plated at a density of 1 × 10^5 cells/mL and, at the moment of collecting samples the cell density was 1 × 10^6 cells/mL approximately. HT-29 cells were routinely plated at a sub-confluent density of 10–15%, at moment of collecting samples cell confluence was always lower than 80%. Unless otherwise indicated, the viability was > 95% in all experiments as assayed by the trypan-blue exclusion method. Cell proliferation and morphology were monitored on a Nikon contrast phase microscope (Eclipse TS100) and

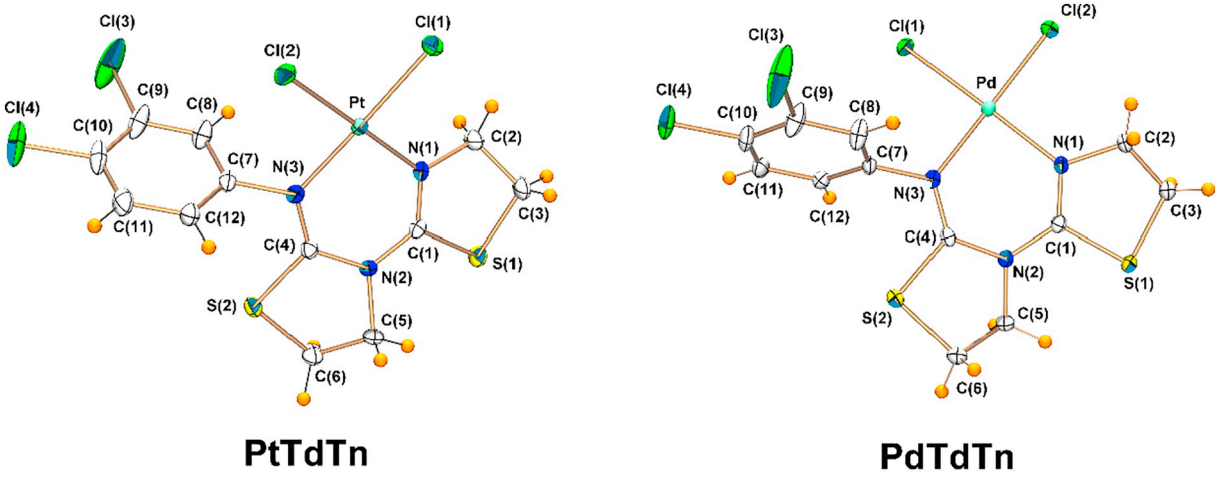

Fig. 1. Crystal structures of PtTdTn and PdTdTn.

photographed using a digital Nikon camera (DS-Qi1Mc).

2.7. Cell treatment

HT-29 cells at a confluence of 40% or U-937 cells at 0.5×10^6 cell/mL were treated with CisPt, TdTn, PtTdTn, PdTdTn or vehicle for 24 h at the indicated concentrations. DMF was used as vehicle and the final DMF concentration did not exceed 0.1% (v/v).

2.8. Cell viability assay

Cell viability was evaluated using the MTT (3-(4,5-dimethylthiazol-2-yl)-2,5-diphenyltetrazolium bromide) metabolic activity assay, which is based on the ability of viable cells to convert a water-soluble, yellow tetrazolium salt into a water-insoluble, purple formazan product. The enzymatic reduction of the tetrazolium salt happens only in living, metabolically active cells, but not in dead cells. After the treatments, the medium was removed and MTT was added into each well, and then incubated for 60 min at 37 °C, as previously described [43]. The supernatant was discarded and DMSO was added to dissolve the formazan crystals. Treatments were carried out in triplicate. Optical density was measured in an automatic microplate reader (Infinite M200, Tecan Austria GmbH, Groedig, Austria) at a test wavelength of 490 nm and a reference wavelength of 650 nm to nullify the effect of cell debris. Data are presented as fold increase versus control (untreated samples).

2.9. Caspase activity

To determine caspase-3, -8 and -9 activity, the measurement of DEVD-AMC cleavage for caspase-3, IEPD-AMC for caspase-8 or LETD-AMC for caspase-9 was performed using a fluorometric assay. Briefly, treated cells were pelleted and washed once with PBS. After centrifugation, cells were resuspended in PBS at a concentration of 2×10^6 cells/100 µL; 25 µL of the suspension were added to a microplate and mixed with the appropriate peptide substrate dissolved in a standard caspase-3/-8 reaction buffer (100 mM HEPES, 10% sucrose, 5 mM DTT, 0.001% NP-40 and 0.1% CHAPS, pH 7.25) or caspase-9 reaction buffer (100 mM MES, 10% PEG, 5 mM DTT, 0.001% NP-40 and 0.1% CHAPS, pH 6.5). Cleavage of the fluorogenic peptide substrate was monitored by AMC liberation in an automatic microplate reader (Infinite M200) with excitation wavelength of 360 nm and emission at 460 nm. Data were calculated as the slope of the line of fluorescence units/mg protein and presented as fold increase over the control level (experimental/control).

2.10. Intracellular ROS production

To quantify the intracellular ROS (Reactive Oxygen Species) generation treated cells were pelleted, wash in PBS and loaded with 2 µM 2′,7′-dichlorodihydrofluorescein diacetate (H2DCFDA) by incubation at 37 °C for 30 min, as previously described [44]. This probe is a non-fluorescent cell-permeable compound, whose acetate groups are dissociated by intracellular esterases and subsequently oxidized. Thus, the non-fluorescent H2DCFDA is converted to 2′,7′-dichlorofluorescein (DCF), which is highly fluorescent and positively correlated with ROS generation. The fluorescence intensity of DCF was measured in an automatic microplate reader (Tecan Infinite M200). Excitation was set at 488 nm and emission at 530 nm. Treatments were carried out in triplicate. Data are presented as fold increase over the pretreatment level (experimental/control).

2.11. Statistical analysis

Data are presented as mean ± standard error of mean (S.E.M) for each group. To compare the different treatments, statistical significance was calculated by one-way analysis of variance (ANOVA) followed by post hoc Tukey test. $P < 0.05$ was considered to indicate a statistically significant difference.

3. Results

3.1. Crystal structures

The crystal structures of metal complexes consist of monomeric [MCl_2(TdTn)] (M = Pt(II) or Pd(II)) molecules. The molecular structures are shown in Fig. 1 and selected interatomic distances and angles are listed in Table 2. As can be seen, PtTdTn and PdTdTn have the same coordination mode with the metal atoms surrounded by a *core*

Table 2
Selected bond lengths (Å) and angles (°) for PtTdTn and PdTdTn.

PtTdTn	Pt-Cl(1)	2.302(1)	Pt-Cl(2)	2.312(1)
	Pt-N(1)	2.012(4)	Pt-N(3)	2.014(5)
	Cl(1)-Pt-Cl(2)	87.7(1)	Cl(1)-Pt-N(1)	92.6(2)
	Cl(1)-Pt-N(3)	178.2(1)	Cl(2)-Pt-N(1)	178.7(1)
	Cl(2)-Pt-N(3)	91.6(1)	N(1)-Pt-N(3)	88.2(2)
PdTdTn	Pd-Cl(1)	2.309(1)	Pd-Cl(2)	2.297(1)
	Pd-N(1)	2.025(2)	Pd-N(3)	2.035(2)
	Cl(1)-Pd-Cl(2)	88.1(1)	Cl(1)-Pd-N(1)	178.6(1)
	Cl(1)-Pd-N(3)	91.7(1)	Cl(2)-Pd-N(1)	92.6(1)
	Cl(2)-Pd-N(3)	177.7(1)	N(1)-Pd-N(3)	87.7(1)

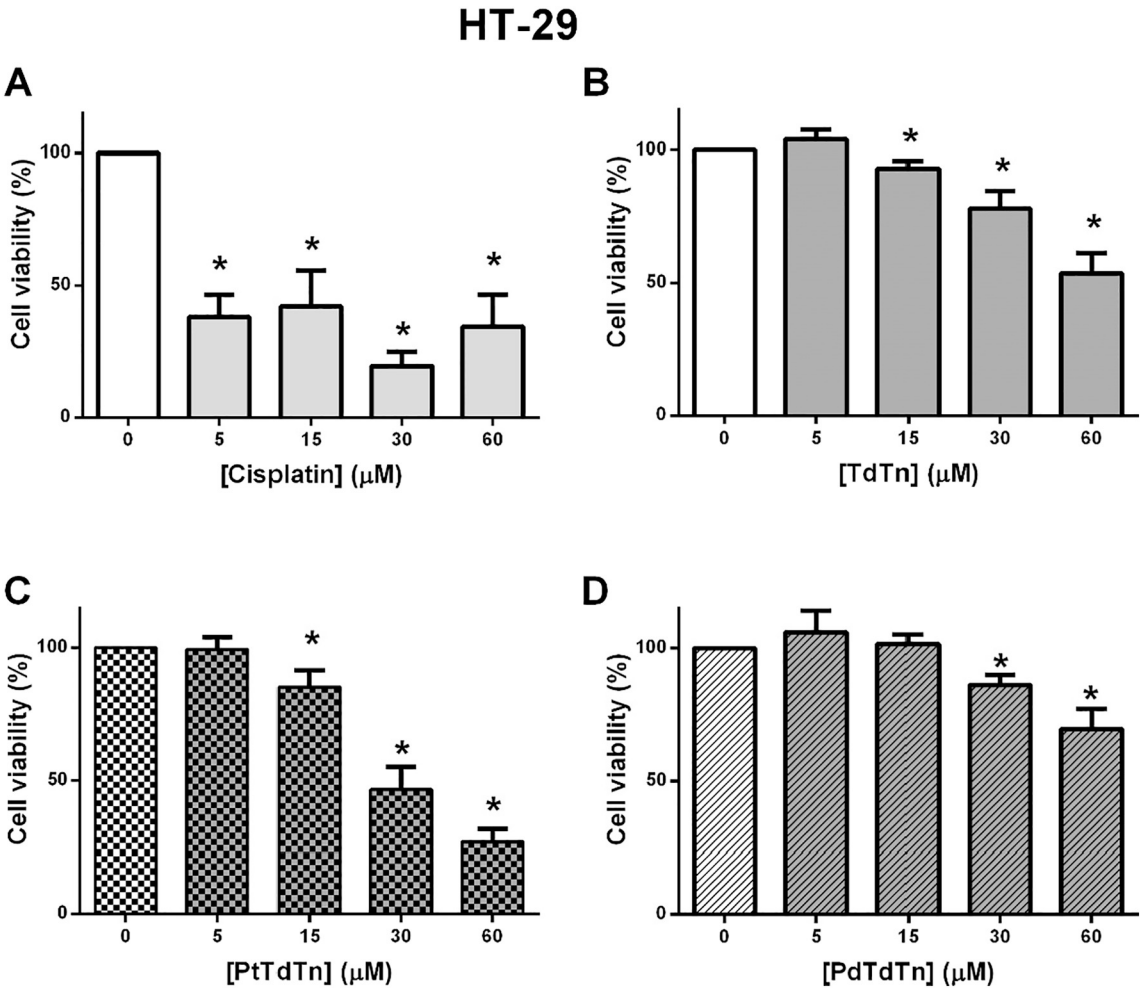

Fig. 2. Effect of thiazoline-based compounds on cell viability in HT-29 cells. Cells were treated for 24 h with compounds [B) TdTn; C) PtTdTn; D) PdTdTn] or cisplatin (A), using the vehicle (DMF) as control. Cell viability was evaluated by means of the MTT assay at different doses (0, 5, 15, 30, 60 μM). Values are presented as means ± SEM of 8 independent experiments and expressed as percentage over the control levels (experimental/control). *$P < 0.05$ compared to control values.

composed of one TdTn coordinated via one imine nitrogen and one thiazoline nitrogen, finishing the coordination of the metal with two chlorine ligands in *cis* disposition. TdTn behaves as a chelated bidentate ligand forming a six-membered metallocycle, which has a configuration near to boat in both complexes. The Pt(II)/Pd(II) atom is located in a slightly distorted square planar coordination geometry (dihedral angle between the planes Cl(1)-M-Cl(2) and N(1)-M-N(3) are 2.2° in PtTdTn and 2.7° in PdTdTn).

The M-Cl bond lengths [Pt-Cl(1) and Pt-Cl(2) in PtTdTn; Pd-Cl(1) and Pd-Cl(2) in PdTdTn] are similar to the calculated average values for squared-planar *cis*-complexes with a Cl_2N_2 coordination environment around M(II) ion [2.298(16) Å for 573 Pt(II) complexes; 2.295(21) Å for 861 Pd(II) complexes], obtained from the Cambridge Structural Database (CSD, Version v5.40, Feb 2019) [45]. Likewise, the M-N_{imine} bond distances are in the same order as the mean values calculated for squared-planar complexes with a Cl_2N_2 coordination environment around M(II) ion [2.011(14) Å for 81 Pt(II) complexes; 2.033(30) Å for 81 Pd(II) complexes] in CSD [45]. Finally, the M-$N_{thiazoline}$ bond distances are slightly shorter than mean values calculated for this type of bonds in CSD [45]: 2.109(21) Å for 2 Pt(II) complexes and 2.067(61) Å for 8 Pd(II) complexes.

It is important to mention that thiazoline ring in metal complexes rotate around C(1)-N(2) bond in such a way that the N(1) and N(3) atoms are on the same side in order to coordinate to metal(II) ions. This is demonstrated by the values of the correspondent torsion angles: S(1)-C(1)-N(2)-C(5) = 18.6° in PtTdTn, −18.8° in PdTdTn; −175.6° in free TdTn [35].

With respect to supramolecular arrangement, the structure is stabilized by Van der Waals forces, not being possible the existence of π-π stacking interactions between phenyl rings.

With the Powder X-ray Diffraction data we carry out LeBail refinements with Topas software [46] to establish the purity of samples. In Fig. S1 it can be seen that the samples are pure. Refined unit cells were obtained with values of a = 9.04, b = 9.03, c = 11.52, α = 101.32, β = 89.58, γ = 111.33, *V* = 856.26, sample displacements = −0.32 mm for compound PtTdTn, and of a = 9.05, b = 9.09, c = 11.59, α = 78.09, β = 88.87, γ = 68.49, V = 867.07, sample displacements = −0.44 mm for compound PdTdTn.

3.2. Spectroscopic studies

A comparison of the ^{1}H NMR spectral data for TdTn and its complexes is shown in Table S1. From these results it can be observed that all ^{1}H NMR signals in both complexes are shifted to downfield respect to the free ligand. This observed difference indicates that in complexes the organic ligand is coordinated to metal ion in DMF solution.

The small values of the shift (0.0–0.4 ppm) are due to the weak Lewis acidity of Pt(II) and Pd(II) ions, except for the corresponding signals to CH_2-$N_{thiazoline}$ that present a larger downfield shift (0.77 ppm in Pt(II) complex and 0.63 ppm in Pd(II) complex). These results suggest the coordination on the thiazoline ring through the nitrogen atom to the metal ion. Likewise, these values show that the metal complexes

are stable in DMF solution and they maintain their identity.

The IR spectra of complexes PtTdTn and PdTdTn (Figs. S2–S5) showed a strong $\nu(C{=}N)_{imine}$ absorption (at 1607 cm^{-1} in PtTdTn and at 1612 cm^{-1} in PdTdTn). These bands are shifted negatively relative to the uncoordinated imine function of the respective ligand (1635 cm^{-1}). Likewise, the in-plane stretching vibrations corresponding to $W_1[\nu(C{=}N)]$ skeletal vibration of the heterocyclic ring was also shifted to lower wavenumbers compared with that of the respective free ligand. Consequently, a coordination via the imine and thiazoline nitrogens of the ligands can be deduced [36].

In the low-frequency region, the C_1 symmetry of PtTdTn and PdTdTn complexes predicts the appearance of four bands assignable to metal–ligand stretching vibrations. The ν(Pt-Cl) and ν(Pd-Cl) vibrations registered at 320 cm^{-1} in PtTdTn and 322 cm^{-1} in PdTdTn, respectively, are in good agreement with literature data [47–49]. In the same way, the bands at 441 cm^{-1} in PtTdTn and 439 cm^{-1} in PdTdTn can be attributed to $\nu(M\text{-}N_{imine})$ vibrations [50–52], while the bands detected at 258 and 215 cm^{-1} in PtTdTn and 256 and 217 cm^{-1} in PdTdTn are assigned to $\nu(M\text{-}N_{thiazoline})$ vibrations [47–53].

3.3. Biological studies

To study the anticancer activity of PtTdTn and PdTdTn compounds, we chose two representative cell lines, HT-29 and U-937 cells. The human colon adenocarcinoma HT-29 cells exemplifies solid tumors; in parallel, human histiocytic lymphoma U-937 cells, classified as monocytic leukemia cell line, represents the hematologic malignancies. First, we first studied the viability of HT-29 and U-937 cells (Figs. 2 and 3, respectively). For this aim, cells were treated for 24 h with PtTdTn and PdTdTn compounds, their ligand TdTn, and cisplatin, which was used as treatment of reference at increasing doses (0, 5, 15, 30, 60 μM). As shown in Fig. 2, the treatments induced a dose-dependent decrease of viability quantified by MTT assay, reaching a statistical significance ($P < 0.05$) for concentrations ≥15 μM PtTdTn (Fig. 2C) and ≥30 μM PdTdTn (Fig. 2D). The treatment with cisplatin significantly decreased ($P < 0.05$) the viability of HT-29 (Fig. 2A) as it is widely known [43], although it did not show a clear dose-dependent effect.

Similarly, cell viability was analyzed in U-937 cells under PtTdTn and PdTdTn treatments. In the same way that HT-29 cells, the cell viability of U-937 cells decreased following a dose-dependent pattern (Fig. 3C and D). However, 5 μM PtTdTn or PdTdTn for 24 h was enough to cause a significant drop of viability ($P < 0.05$) (Fig. 3C and D, respectively). U-937 cells displayed an augmented response to these drugs regarding to HT-29 cells. This fact could be explained in the context of the mechanism of rapid apoptosis, which is characteristic of monocytes [54]. The complexes of Pt(II) and Pd(II) induce apoptosis by interfering with the replication fork of proliferating cells [10,55]. The high sensitivity of U-937 cells to these compounds in an independent manner of DNA damage could make the difference and evidence a remarkable contrast between HT-29 and U-937 cells to PtTdTn and PdTdTn in terms of viability.

Interestingly, not only PtTdTn and PdTdTn, but also the ligand TdTn by itself showed anticancer activity in both cell lines in a dose-dependent manner, although TdTn was shown to be more effective upon U-

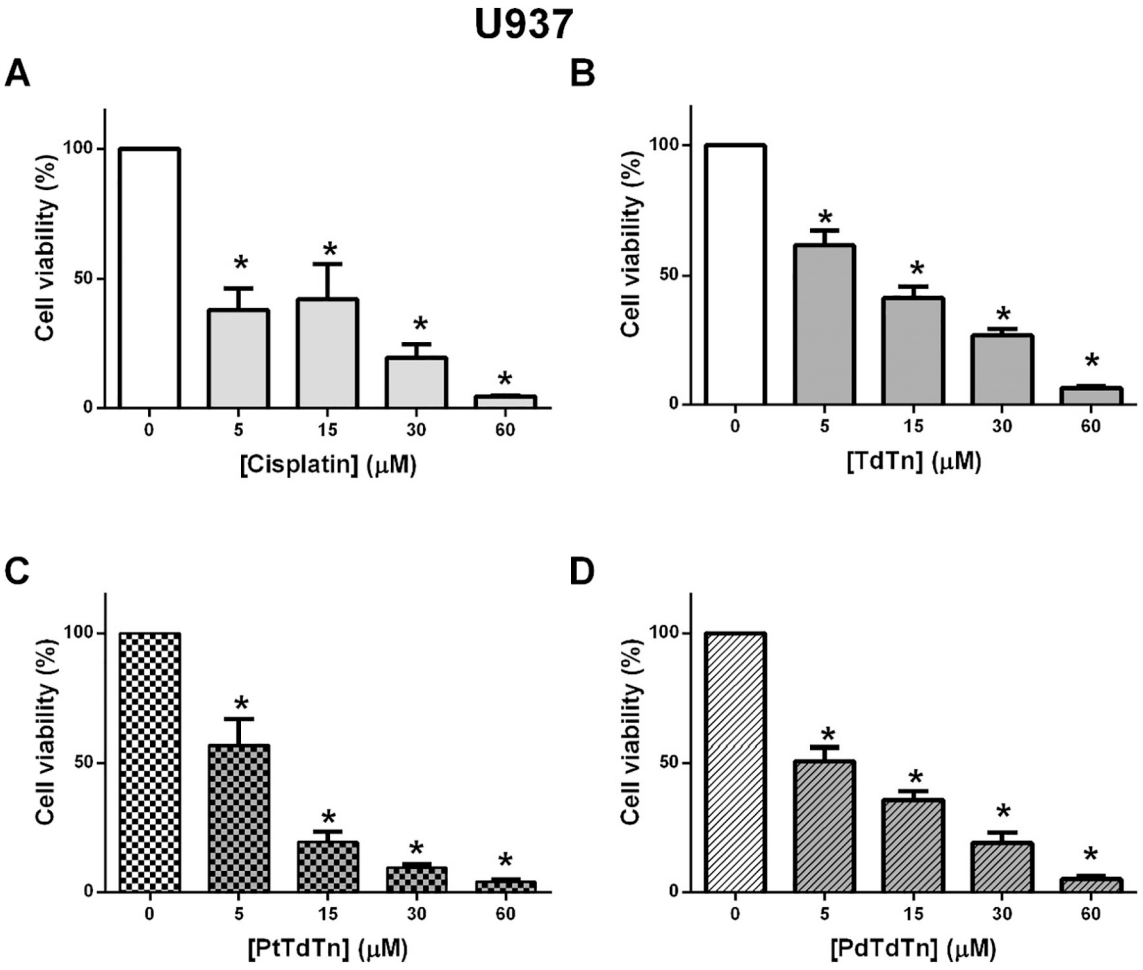

Fig. 3. Effect of thiazoline-based compounds on cell viability in U-937 cells. Cells were treated for 24 h with compounds [B) TdTn; C) PtTdTn; D) PdTdTn] or cisplatin (A), using the vehicle (DMF) as control. Cell viability was evaluated by means of the MTT assay at different doses (0, 5, 15, 30, 60 μM). Values are presented as means ± SEM of 8 independent experiments and expressed as percentage over the control levels (experimental/control). *$P < 0.05$ compared to control values.

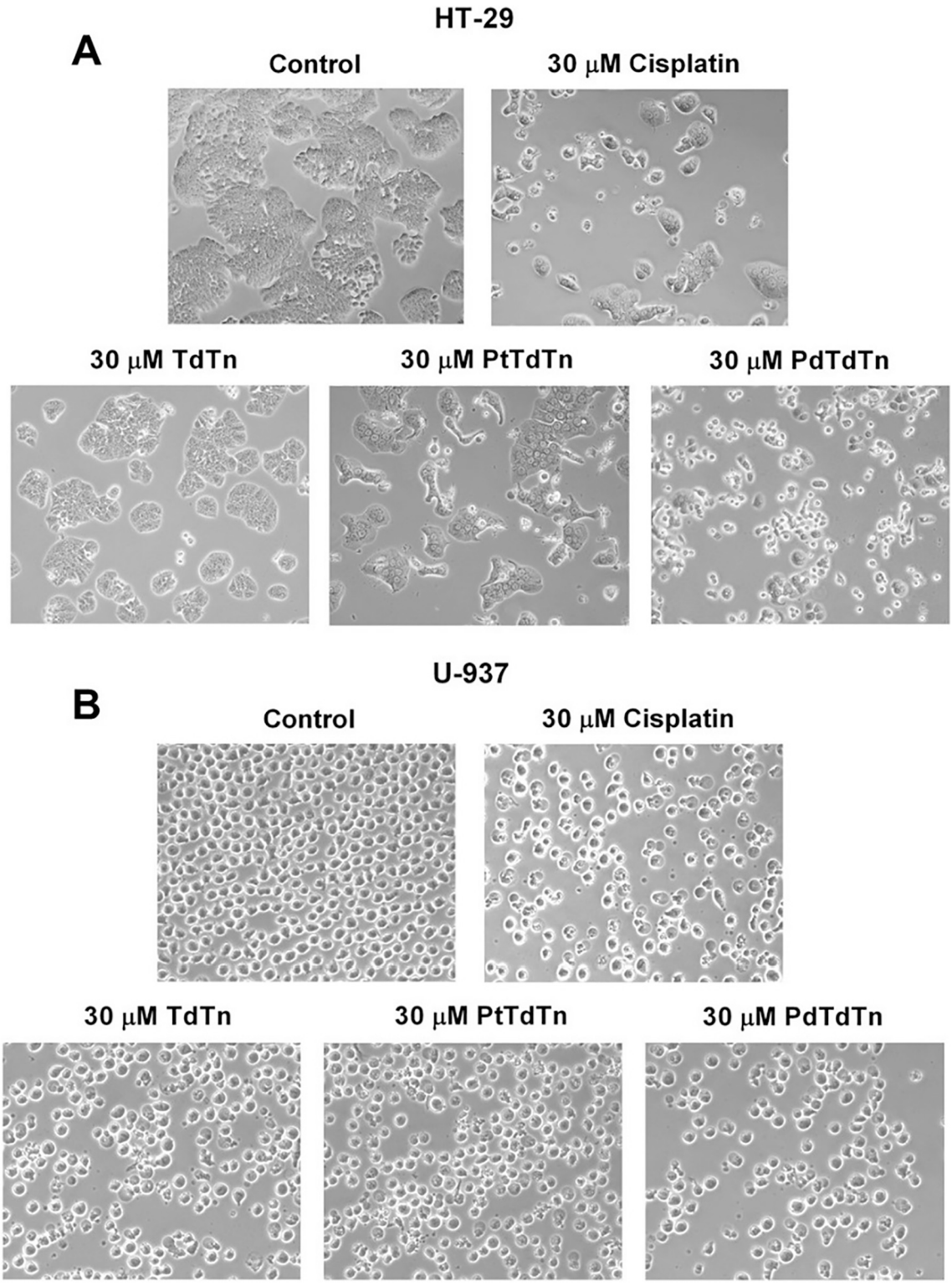

Fig. 4. Effect of thiazoline-based compounds on cell proliferation in (A) HT-29 and (B) U-937 cells. Cells were treated for 24 h with 30 μM compounds [TdTn; PtTdTn; PdTdTn] or 30 μM cisplatin, using the vehicle (DMF) as control. Cells were visualized on a Nikon Eclipse TS 100 contrast phase microscope and the images were captured using a digital Nikon (DSQi1Mc) camera, and a representative field of each experimental group is shown.

937 cells. This is the very first time that this particular ligand has been shown to have antitumor effects and, therefore, the certainty about the mechanisms that could be involved in the antitumor properties of TdTn are unknown. Similar structures, as synthetic oligomers derived from 2-thiazoline, have been described to inhibit tumor cells [24]. Curacin-A that contains thiazoline in its structure has been shown to interact with colchicine binding site in microtubules avoiding tubulin polymerization in cancer cells [26]. Thiazole derivatives have also displayed to interfere with cell cycle and produce DNA fragmentation and mitochondrial depolarization in five tumor cell lines [56]. On the other hand, in wide spectrum of cancer cells prohibitins (involved in cell viability) were shown to interact with new small molecules that contain thiazoline

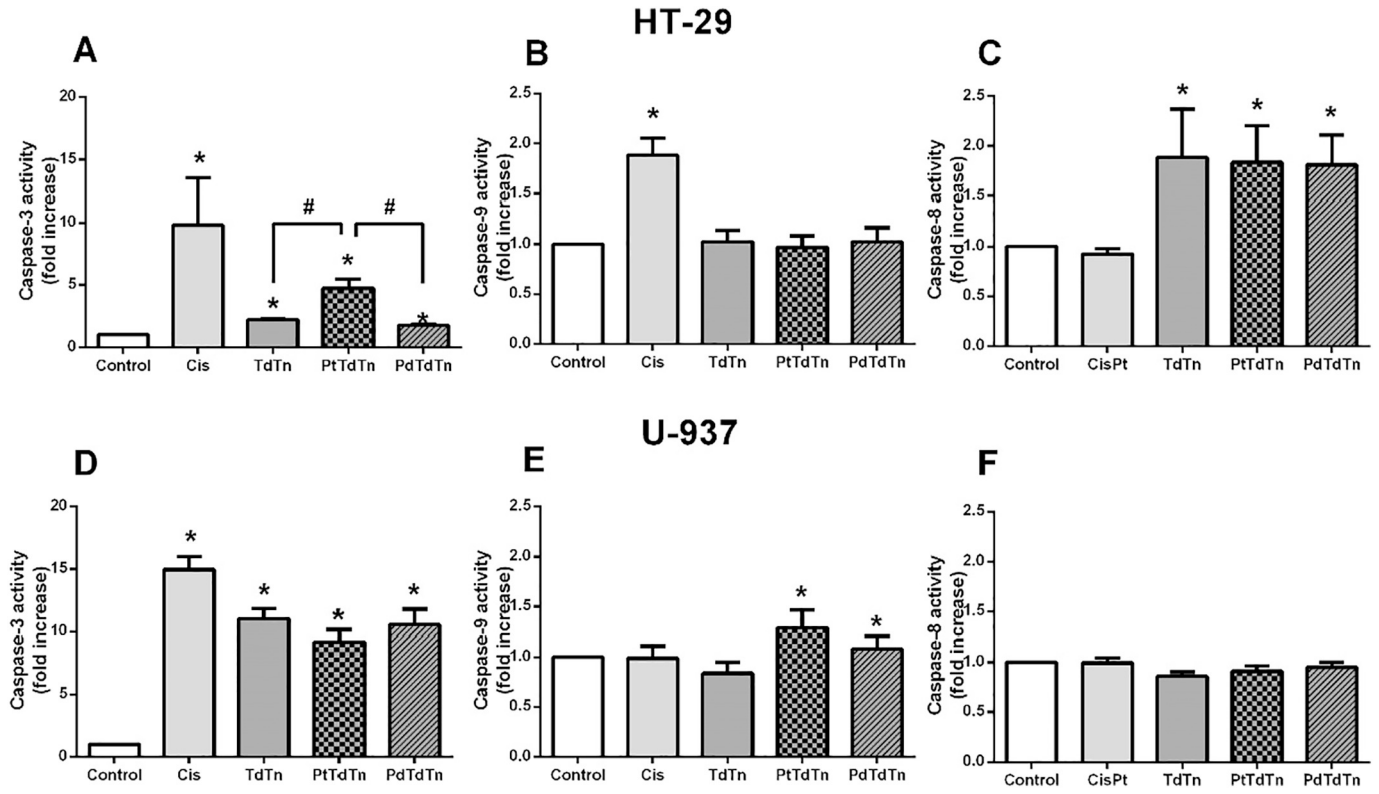

Fig. 5. Effect of thiazoline-based compounds on caspase-3, -9 and -8-activity in HT-29 (A, B, C, respectively) and U-937 cells (C, D, E, respectively). Cells were treated for 24 h with 30 μM compounds [TdTn; PtTdTn; PdTdTn] or 30 μM cisplatin, using the vehicle (DMF) as control. Caspase-3, -8 and -9 enzymatic activities were estimated as described under Material and Methods. Values are presented as means ± SEM of 4–8 independent experiments and expressed as fold increase over the control level (experimental/control). *$P < 0.05$ compared to control values.

molecules [57].

Cancer therapies aim to inhibit cell proliferation as a strategy to hamper progression, and even dissemination of tumors. Thiazole is a structure integrated in many anticancer drugs presenting different strategies to inhibit cell growth and proliferation. In this way, the BCR/ABL (Breakpoint Cluster Region/ABelson murine Leukemia viral oncogene homolog) inhibitor dasatinib is used for cases of chronic leukemia [57] by inhibiting T-cells receptor-mediated proliferation; recently, newly synthesized candidates that are using thiazole structures are showing successful results as anticancer agents with EGFR (Epidermal Growth Factor Receptor) inhibitory activity in a variety of tumor cell lines [58]. The compounds presented herein aim to combine the Pt and Pd ability to interfere with the synthesis of DNA via the inhibitory capacities of thiazole. Fig. 4 shows microscopy images both cell cultures, U-937 (Fig. 4A) and HT-29 (Fig. 4B), after treatments. PtTdTn and PdTdTn induced a decrease in confluence of the cultures (Fig. 4), what agrees with the results of cell viability described above. It is important to note that 30 μM TdTn (ligand) reduced the confluence of U-937 and HT-29 cells with respect to the control growths, therefore this fact evidences a clear activity of the ligand which was extended to both cell lines. Nonetheless, the treatment with 30 μM PtTdTn or 30 μM PdTdTn during 24 h, in both cell lines, diminished the confluence of the cell culture further than the capacity of the ligand alone.

Caspases are cysteinyl-aspartate proteases involved and activated mainly in apoptotic cell death processes. Caspase activities are analyzed as indicators of activation of the two major routes of apoptosis, traditionally named intrinsic and extrinsic. Caspase-8 and -9 are initiators of the extrinsic and intrinsic pathway, respectively. Both routes converge in the activation of the executioner caspase-3. When HT-29 cells were treated with 30 μM PtTdTn or 30 μM PdTdTn for 24 h, caspase-3 activity showed a significant increase ($P < 0.05$, Fig. 5A) regarding to the control values; interestingly, 30 μM TdTn also promoted caspase-3 activation ($P < 0.05$, Fig. 5A). Although PtTdTn and PdTdTn compounds, or the ligand, did not reach the values of activation induced by cisplatin. Nonetheless, PtTdTn was able to promote an additional increase of caspase-3 activation compared to PdTdTn or ligand alone values ($P < 0.05$, Fig. 5A), what agrees with results of cellular viability (Fig. 2C, D). Despite 30 μM cisplatin induced a significant increase of caspase-9 activation, the effect of Pt(II) and Pd(II) or the ligand were negligible ($P < 0.05$, Fig. 5B). On the contrary, cisplatin did not show effect at modulating caspase-8 activity, while TdTn, PtTdTn and PdTdTn promoted a substantial rise ($P < 0.05$, Fig. 5C).

These results show a profile of caspase-3 activation for all of the treatment which agrees with cell viability assay carried out in HT-29 cells. However, in the light of these results, the apoptosis signaling was not processed by the same pathway. Thus, the mechanisms that activated the apoptosis induced by thiazoline compounds involved the extrinsic pathway via activation of caspase-8. On the contrary the apoptotic cell death induced by cisplatin involved the intrinsic pathway, this point renders reasonable to believe that cisplatin activates a DNA damage signaling cascade that includes mitochondrial apoptotic molecules.

Intriguingly, the pattern of activation of caspase-3, -9 and -8 emerging from the treatment of U-937 cells turned out completely different from that of HT-29 cells. When U-937 cells were treated with 30 μM PtTdTn or 30 μM PdTdTn during 24 h, caspase-3 activity showed a significant increase ($P < 0.05$, Fig. 5D). However, no significance was found between the ligand and each of the metallic compounds. Therefore, it is logical to think that caspase-3 activation induced by these thiazoline compounds is independent of the metallic atom of the structure, and that the main involvement of caspase-3 activation is carried out by TdTn ligand. On the contrary, only the treatments of 30 μM PtTdTn and PdTdTn for 24 h caused caspase-9 activation in U-937 cells (Fig. 5D), suggesting that the metallic atoms played a crucial

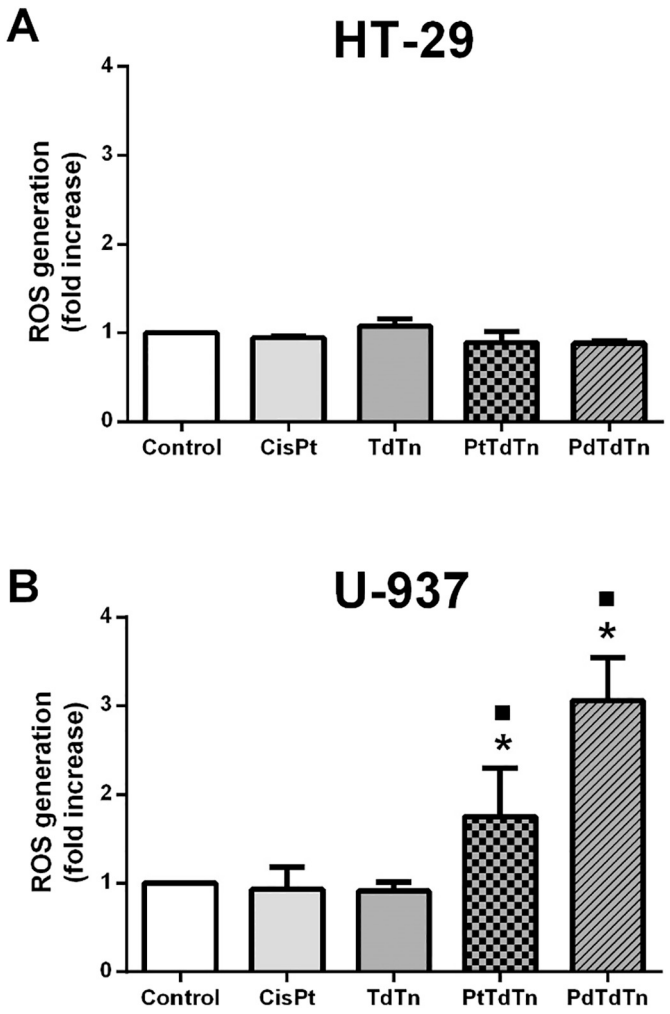

Fig. 6. Effect of thiazoline-based compounds on ROS generation in (A) HT-29 and (B) U-937 cells. Cells were treated for 24 h with 30 μM compounds [TdTn; PtTdTn; PdTdTn] or 30 μM cisplatin, using the vehicle (DMF) as control. ROS generation were estimated as described under Material and Methods. Values are presented as means ± SEM of 6–8 independent experiments and expressed as fold increase over the control level (experimental/control). *$P < 0.05$ compared to control values. *$P < 0.05$ compared to TdTn values.

role in caspase-9 activation in U-937 cells. Cisplatin or TdTn alone, in the same conditions of concentration and time did not modulate caspase-9 activity (Fig. 5E). Caspase-8 did not undergo any modulation after any of the treatments (Fig. 5F).

Finally, we analyzed the intracellular ROS generation as a marker of apoptosis to evaluate its contribution on apoptotic cell death of U-937 and HT-29 treated with our compounds. Our drugs caused undetectable effects on intracellular ROS generation in HT-29 cells (Fig. 6A). However, in U-937 cells, PtTdTn and PdTdTn caused a significant increase ($P < 0.05$, Fig. 6B). The main intracellular source of ROS, but not the only one, is the mitochondrion, and this profile of ROS generation induced by thiazoline compounds is narrowly in coherence with the profile of caspase-9 activation. In other words, only those treatments that promoted intracellular ROS generation were able to induce caspase-9 activation in U-937 cells. It is also worthy to comment that cisplatin induced caspase-9 activation without ROS generation in HT-29 cells, perhaps because the intracellular ROS generation was undetectable in our experimental conditions, but these findings agree with what we have seen in previous results, where we additionally showed that melatonin enhances the pro-apoptotic effects of cisplatin in HT-29 cells [59].

4. Conclusions

The goal of the synthesis of many anticancer agents is to hamper cancer cells' proliferation to beat the metastatic processes [60]. In the path to this aim, cancer cells undergo frequently undesirable responses to the anticancer drugs such as resistance acquisition. On the other hand, anticancer agents might be harmful for healthy cells, and different tissues are sensitive to certain treatments, as renal toxicology has been widely described [61]. Then, resistance acquisition and side effects stablish the front to fight against cancer with a wider palette of alternative anticancer drugs ready to substitute those drugs that are not working as expected. Herein, we have demonstrated how our compounds, not only have diminished the proliferation capacity, but also have evoked the apoptotic process in both cellular types assayed. Previous studies in the literature suggest that these compounds might develop an antitumor action by multiple targets. On the one hand, Pt(II) and Pd(II) can interact with nucleotides making up DNA-Pt or DNA-Pd adducts hindering the cell cycle progression or even activating the DNA damage response [62]. On the other hand, thiazoline derivatives seem to perform their antitumor action through several target [56,57,60]. This study supposes the first approach to describe the synthesis and apoptotic effects of compounds PtTdTn and PdTdTn. Further studies are required to unveil the mechanisms activated by these compounds to beat the cancer cells and the resistance that different pathways or different cancer type could show against them.

Abbreviations

AML	acute myeloid leukemia
CHAPS	3-[(3-Cholamidopropyl)dimethylammonio]-1-propanesulfonate
CisPt	cisplatin
CSD	Cambridge Structural Database
CTR1	human copper transporter 1
DMF	*N,N*-dimethylformamide
DMSO	dimethyl sulfoxide
EGFR	epidermal growth factor receptor
ERCC1	DNA excision repair protein
FBS	fetal bovine serum
GSH	glutathione
HEPES	4-(2-hydroxyethyl)-1-piperazineethanesulfonic acid
HT-29	human colon adenocarcinoma
MES	4-Morpholineethanesulfonic acid
MTT	3-(4,5-dimethylthiazol-2-yl)-2,5-diphenyltetrazolium bromide
NER	nucleotide excision repair
ROS	reactive oxygen species
RPMI	Roswell Park Memorial Institute
TdTn	2-(3,4-dichlorophenyl)imino-N-(2-thiazolin-2-yl)thiazolidine
U-937	human histiocytic lymphoma

Declaration of competing interest

The authors declare that they have no known competing financial interests or personal relationships that could have appeared to influence the work reported in this paper.

Acknowledgements

Authors thank José Antonio Pariente, Ana Beatriz Rodríguez, Álvaro Bernalte and Fernando J. Barros for their laboratory and material to carry out the experiments, as well as their expert revising. Supported by Junta de Extremadura-FEDER (IB18013, GR18040 and GR18062) and "Asociación Oncológica Tierra de Barros" and "Asociación Oncológica Esperanza de Vida". J. Espino holds a post-doctoral fellowship financed by Ministerio de Ciencia, Innovación y Universidades (IJCI-2016-28030).

Appendix A. Supplementary data

Supplementary data to this article can be found online at https://doi.org/10.1016/j.jinorgbio.2019.110870.

References

[1] K. Fernald, M. Kurokawa, Trends Cell. Biol. 23 (2013) 620–633.
[2] S. Fulda, Int. J. Cancer 124 (2009) 511–515.
[3] World Health Organization. www.who.int/mediacentre/factsheets/fs297/en/ (Accessed May 21, 2018).
[4] World Health Organization. International Agency for Research on Cancer. Global Cancer Observatory. gco.iarc.fr/today/online-analysis-multi-bars?mode=cancer&mode_population=continents&population=900&sex=0&cancer=29&type=1&statistic=0&prevalence=0&color_palette=default (Accesed May 21, 2018).
[5] B.B. Zeisig, A.G. Kulasekararaj, G.J. Mufti, C.W. So, Cancer Cell 22 (2012) 698–698.e1.
[6] A. Zebisch, S. Hatzl, M. Pichler, A. Wölfler, H. Sill, Int. J. Mol. Sci. 17 (2016) 2080.
[7] T.W. Hambley, Coord. Chem. Rev. 166 (1997) 181–223.
[8] N.J. Wheate, S. Walker, G.E. Craig, R. Oun, Dalton Trans. 39 (2010) 8113–8127.
[9] E.R. Jamieson, S.J. Lippard, Chem. Rev. 99 (1999) 2467–2498.
[10] C. Barckhausen, W.P. Roos, S.C. Naumann, B. Kaina, Oncogene 33 (2013) 1964–1974.
[11] K.D. Ivy, J.H. Kaplan, Mol. Pharmacol. 83 (2013) 1237–1246.
[12] I.S. Song, N. Savaraj, Z.H. Siddik, P. Liu, Y. Wei, C.J. Wu, M.T. Kuo, Mol. Cancer Ther. 3 (2004) 1543–1549.
[13] B. Köberle, M.T. Tomicic, S. Usanova, B. Kaina, Biochim. Biophys. Acta 1806 (2010) 172–182.
[14] H.Y. Chen, C.J. Shao, F.R. Chen, A.L. Kwan, Z.P. Chen, Int. J. Cancer 126 (2010) 1944–1954.
[15] E.C. Friedberg, A. Aguilera, M. Gellert, P.C. Hanawalt, J.B. Hays, A.R. Lehmann, T. Lindahl, N. Lowndes, A. Sarasin, R.D. Wood, DNA Repair 5 (2006) 989–996.
[16] H.W. Lee, Y.W. Choi, J.H. Han, J.H. Kim, J.H. Jung, S.H. Jeong, S.Y. Kang, J.H. Choi, Y.T. Oh, K.J. Park, S.C. Hwang, S.S. Sheen, Lung Cancer 65 (2009) 377–382.
[17] Y.P. Liu, Y. Ling, Q.F. Qi, Y.P. Zhang, C.S. Zhang, C.T. Zhu, M.H. Wang, Y.D. Pan, Oncol. Lett. 5 (2013) 935–942.
[18] M. Dabholkar, J. Vionnet, F. Bostick-Bruton, J.J. Yu, E. Reed, J. Clin. Invest. 94 (1994) 703–708.
[19] R. Rossell, M. Taron, A. Barnadas, G. Scargliotti, C. Sarries, B. Roig, Cancer Control 10 (2003) 297–305.
[20] J. Mendoza, J. Martínez, C. Hernández, D. Pérez-Montiel, C. Castro, E. Fabián-Morales, M. Santibáñez, R. González-Barrios, J. Díaz-Chávez, M.A. Andonegui, N. Reynoso, L.F. Oñate, M.A. Jiménez, M. Núñez, R. Dyer, L.A. Herrera, Br. J. Cancer 109 (2013) 68–75.
[21] C.A. Rabik, M.E. Dolan, Cancer Treat. Rev. 33 (2007) 9–23.
[22] W.J. Wu, Y. Zhang, Z.L. Zeng, X.B. Li, K.S. Hu, H.Y. Luo, J. Yang, P. Huang, R.H. Xu, Biochem. Pharmacol. 85 (2013) 486–496.
[23] Z.A. Alsharif, M.A. Alam, RSC Adv 7 (2017) 32647–32,651.
[24] F.S. Han, H. Osajima, M. Cheung, H. Tokuyama, T. Fukuyama, Chem. Eur. J. 13 (2007) 3026–3038.
[25] J. Lai, J. Yu, B. Mekonnen, J. Falck, Tetrahedron Lett 37 (1996) 7167–7170.
[26] Z. Chang, N. Sitachitta, J.V. Rossi, M.A. Roberts, P.M. Flatt, J. Jia, D.H. Sherman, W.H. Gerwick, J. Nat. Prod. 67 (2004) 1356–1367.
[27] F.E. Onen-Bayram, I. Durmaz, D. Scherman, J. Herscovici, R. Cetin-Atalay, Bioorg. Med. Chem. 20 (2012) 5094–5102.
[28] R. Romagnoli, P.G. Baraldi, M.K. Salvador, M.E. Camacho, J. Balzarini, J. Bermejo, F. Estévez, Eur. J. Med. Chem. 63 (2013) 544–547.
[29] C.A. Bolos, K.T. Papazisis, A.H. Kortsaris, S. Voyatzi, D. Zambouli, D.A. Kyriakidis, J. Inorg. Biochem. 88 (2002) 25–36.
[30] A.Th. Chaviara, P.C. Christidis, A. Papageorgiou, E. Chrysogelou, D.J. Hadjipavlou-Litina, C.A. Bolos, J. Inorg. Biochem. 99 (2005) 2102–2109.
[31] J. Dehand, J. Jordanov, J.P. Beck, Chem. Biol. Interact. 11 (1975) 605–609.
[32] A.R. Kapdi, I.J.S. Fairlamb, Chem. Soc. Rev. 43 (2014) 4751–4777.
[33] T. Lazarevic, A. Rilak, Z.D. Bugarcic, Eur. J. Med. Chem. 142 (2017) 8–31.
[34] F.J. Barros-García, A. Bernalte-García, A.M. Lozano-Vila, F. Luna-Giles, E. Viñuelas-Zahínos, Polyhedron 24 (2005) 129–136.
[35] F.J. Barros-García, A. Bernalte-García, A.M. Lozano-Vila, F. Luna-Giles, J.A. Pariente, R. Pedrero Marín, A.B. Rodríguez, J. Inorg. Biochem. 100 (2006) 1861–1870.
[36] A.M. Lozano-Vila, F. Luna-Giles, E. Viñuelas-Zahínos, F.L. Cumbrera, A.L. Ortiz, F.J. Barros-García, A.B. Rodríguez, Inorg. Chim. Acta 365 (2011) 282–289.
[37] R.J. Outcalt, J. Heterocycl. Chem. 24 (1987) 1425–1428.
[38] J.H. Price, A.N. Williamson, R.F. Schramm, B.B. Wayland, Inorg. Chem. 11 (1972) 1280–1284.
[39] Bruker, A.X.S. Inc. SADABS, Bruker, A.X.S. Inc., Madison, WI, 2012.
[40] M. Sheldrick, SHELXS-14, Program for Crystal Structures Solution, University of Göttingen, Germany, 2014.
[41] G.M. Sheldrick, Crystal structure refinement with SHELXL, Acta Cryst C71 (2015) 3–8.
[42] L.J. Farrugia, J. Appl. Cryst. 32 (1999) 837–838.
[43] R. Pariente, I. Bejarano, J. Espino, A.B. Rodríguez, J.A. Pariente, Cancer Chemother. Pharmacol. 80 (2017) 985–998.
[44] A.C. Uguz, B. Cig, J. Espino, I. Bejarano, M. Naziroglu, A.B. Rodríguez, J.A. Pariente, J. Pineal Res. 53 (2012) 91–98.
[45] I.J. Bruno, J.C. Cole, P.R. Edgington, M. Kessler, C.F. Macrae, P. McCabe, J. Pearson, R. Taylor, Acta Crystallogr. B. 58 (2002) 389–397.
[46] Topas-R, Bruker AXS: General profile and structure analysis software for powder diffraction data.
[47] J.R. Ferraro, Low-frequency Vibrations of Inorganic and Coordination Compounds, Springer Plenum Press, New York, 1971.
[48] K. Nakamoto, Infrared and Raman Spectra of Inorganic and Coordination Compounds, 3rd ed., Wiley & Sons, New York, 1978.
[49] U. Belluco, F. Benetollo, R. Bertani, G. Bombieri, R.A. Michelin, M. Mozzon, A.J.L. Pombeiro, M.F.C. Guedes da Silva, Inorg. Chim. Acta 330 (2002) 229–239.
[50] H.A. El-Asmy, I.S. Butler, Z.S. Mouhri, B.J. Jean-Claude, M.S. Emmam, S.I. Mostafa, J. Mol. Struct. 1059 (2014) 193–201.
[51] A. Boixassa, J. Pons, X. Solans, M. Font-Bardía, J. Ros, Inorg. Chim. Acta 357 (2004) 827–833.
[52] B. Shafaatian, A. Soleymanpour, N. Kholghi Oskouei, B. Notash, S.A. Rezvani, Spectrochim. Acta A Mol. Biomol. Spectrosc 128 (2014) 363–369.
[53] J. Dehand, J. Jordanov, Inorg. Chim. Acta 17 (1976) 37–44.
[54] D.F. Mangan, G.R. Welch, S.M. Wahl, J. Immunol. 146 (1991) 1541–1546.
[55] T. Scattolin, I. Caligiuri, L. Canovese, N. Demitri, R. Gambari, I. Lampronti, F. Rizzolio, C. Santo, F. Visentin, Dalton Trans 47 (2018) 13616–13,630.
[56] T.I. de Santana, M.O. Barbosa, P.A.T.M. Gomes, A.C.N. da Cruz, T.G. da Silva, A.C.L. Leite, Eur. J. Med. Chem. 144 (2018) 874–886.
[57] A. Pérez-Perarnau, S. Preciado, C.M. Palmeri, C. Moncunill-Massaguer, D. Iglesias-Serret, D.M. González-Gironès, M. Miguel, S. Karasawa, S. Sakamoto, A.M. Cosialls, C. Rubio-Patiño, J. Saura-Esteller, R. Ramón, L. Caja, I. Fabregat, G. Pons, H. Handa, F. Albericio, J. Gil, R. Lavilla, Angew. Chem. Int. Ed. Engl. 53 (2014) 10150–10,154.
[58] R.F. George, E.M. Samir, M.N. Abdelhamed, H.A. Abdel-Aziz, S.E. Abbas, Bioorg. Chem. 83 (2018) 186–197.
[59] R. Pariente, I. Bejarano, A.B. Rodríguez, J.A. Pariente, J. Espino, Mol. Cell. Biochem. 440 (2018) 43–51.
[60] S. Zheng, Q. Zhong, Q. Jiang, M. Mottamal, Q. Zhang, N. Zhu, M.E. Burow, R.A. Worthylake, G. Wang, ACS Med. Chem. Lett. 4 (2013) 191–196.
[61] B.S. Cummings, R.G. Schnellmann, Pharmacol. Exp. Ther. 302 (2002) 8–17.
[62] V.T. Yilmaz, C. Icsel, M. Aygun, M. Erkisa, E. Ulukaya, Eur. J. Med. Chem. 158 (2018) 534–547.